

Distance Based Decision Fusion in a Distributed Wireless Sensor Network

Marco Duarte and Yu-Hen Hu

University of Wisconsin - Madison
Department of Electrical and Computer Engineering
Madison WI 53706, USA
Email: mfduarte@wisc.edu, hu@engr.wisc.edu
<http://www.ece.wisc.edu/~sensit>

Abstract. Target classification fusion problem in a distributed, wireless sensor network is investigated. We propose a distance-based decision fusion scheme exploiting the relationship between sensor to target distance, signal to noise ratio and classification rate, which requires less communication while achieving higher region classification rate when compared to conventional majority-vote based fusion schemes. Several different methods are tested, and very encouraging simulation results using real world experimental data samples are also observed.

1 Introduction

It will soon become feasible to deploy massive amount of low-cost miniature sensors to monitor large regions over ground surface, underwater, or atmosphere. These sensor nodes will be integrated with miniature power supply, sensors, on-board processors, and wireless radio communication modules, capable of forming a large-scale ad hoc wireless network [3]. Common signal processing tasks performed in a sensor system include event detection, and parameter estimation. While these detection, classification, and tracking algorithms have been well developed for conventional centralized signal processing systems, much less is known for a distributed wireless sensor network system. A distinct feature of such a system is that it contains multiple, physically scattered sensing and processing modules that must collaborate with each other to achieve high performance. Conventional centralized information and data fusion techniques are unsuited for such an application because too much data must be communicated from individual sensors to a centralized fusion center. Instead, a family of novel distributed, localized, and location centric signal processing and information fusion algorithms must be developed to meet this demand.

In this paper, we propose a distance-based decision fusion method for the collaborative target classification of moving vehicles using acoustic spectral features. A key innovation of this approach is to use the distance between the target and the sensor as a parameter to select sensors that give reliable classification result to participate decision fusion. Intuitively, sensors that are far from the

target will have lower probability of making correct classification decisions. This intuitive concept is verified using real world experimental data recorded at a military training ground using a prototype wireless sensor network. In the rest of this paper, the background of wireless sensor network architecture will be introduced in section 2.1. The sensor network signal processing algorithms will be surveyed in section 2.2 with special attention to the task of target classification and its performance with respect to sensor-target distance. The distance-based classification fusion method will be discussed in section 3, completed with simulation results using real world experimental data.

2 Distributed Wireless Sensor Network Signal Processing

2.1 Wireless Sensor Nodes and Network

We assume that a number of sensor nodes are deployed in an outdoor sensor field. Each sensor node consists of an on-board computer, power source (battery), one or more sensors with different modalities, and wireless transceivers. Depicted in Figure 1(a) is a prototype sensor node used in the DARPA SensIT project, manufactured by Sensoria, Inc. With this sensor node, there are three sensing modalities: acoustic (microphone), seismic (geophone), and infrared (polarized IR sensor). The acoustic signal is sampled at 5 kHz at 12 bit resolution. The on-board computer is a 32-bit RISC processor running the Linux operating system.

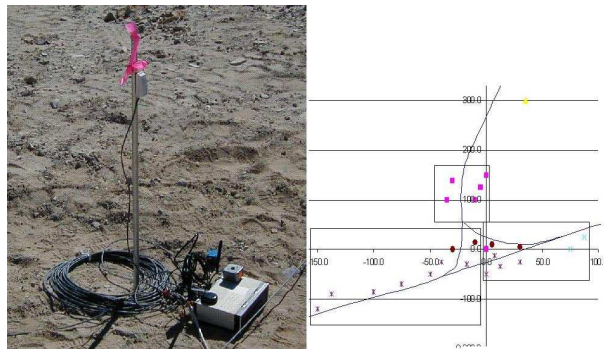


Fig. 1. (a) A Sensoria sensor node, (b) sensor field layout

The sensor field (c.f. Figure 1(b)) is an area of approximately 900×300 meters in a California Marine training ground. The sensors, denoted by dots of different colors in Figure 1(b) are layout along side the road. The separation of adjacent sensors ranges from 20-40 meters. We partition the sensors into three geographically local *regions*. Sensors within each region will be able to communicate freely. One sensor within each region is designated as a *manager node*.

The manager node will be given the authority to communicate with manager nodes of surrounding regions. This hierarchy of communication ensures that only local wireless traffic will be engaged, and hence contributes to the goal of energy conservation.

Military vehicles, including the *Assault Amphibian Vehicle* (AAV), the *Dragon Wagon* (DW), the *High Mobility Multipurpose Wheeled Vehicle* (HMMWV), and others are driving passing through the roads. The objective is to detect the vehicles when they pass through each region. The type of the passing vehicle then will be identified, and the accurate location of that vehicle will be estimated using an *energy-based localization algorithm*. In the following discussion, we will assume there is at most one vehicle in each region. During the experimentation in November 2001, multi-gigabyte data samples have been recorded and are used in this paper. We will call these data Sitex02 data set.

2.2 Sensor Network Signal Processing Tasks

In a distributed wireless sensor network, the bulk of signal processing tasks are distributed over individual nodes. In particular, at each sensor node, the on-board computer will process the sensed acoustic, seismic and PIR data to detect the presence of a potential target, and to classify the type of vehicle that is detected. In this paper, we will focus on the processing of acoustic sensing channel only.

CFAR Target Detection For each of the 0.75 second duration, the energy of the acoustic signal will be computed. This single energy reading then will be fed into a *constant false alarm rate* (CFAR) energy detector [6] to determine whether the current energy reading has a magnitude that exceeds a computed threshold. If so, a *node-detection* event will be declared for this duration. Otherwise, the energy reading is considered as contributions from the background noise.

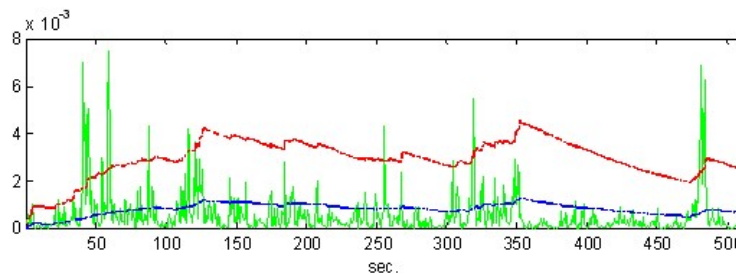


Fig. 2. Illustration of CFAR detection. The upper line is the threshold. Vertical axis is energy. When the energy exceeds the threshold, detection is made

In Figure 2, a sample energy time series is plotted for a period of 500 seconds. The two horizontal lines represent the threshold with two different false alarm rates. These thresholds vary with time as they are updated by the energy readings that do not exceed the thresholds.

From Figure 2, it is clear that when the background noise energy increases, the threshold increases as well. If the signal energy distribution, which is assumed to be unknown in the CFAR detection, remains unchanged, the probability of miss will increase. Furthermore, in this out-door, unrestricted environment, we observe that when the wind-gusts blow directly into the microphone, it often create a surge of false detection events. These anomalies are likely to cause performance degradation.

Target Classification Once a positive target-detection decision has been made, a pattern classifier using Maximum likelihood pattern classifier [6] is invoked. The acoustic signal is recording using a sampling frequency of 4960 Hz. We use a 50 dimensional feature vector based on the Fourier power spectrum of the corresponding acoustic time series within the 0.75-second duration. This feature is created by averaging by pairs the first 100 points of the 512-point FFT, which are then normalized; the resolution of the frequency spectrum sampling is 19.375 Hz due to the averaging. Some typical features can be seen in Figure 3.

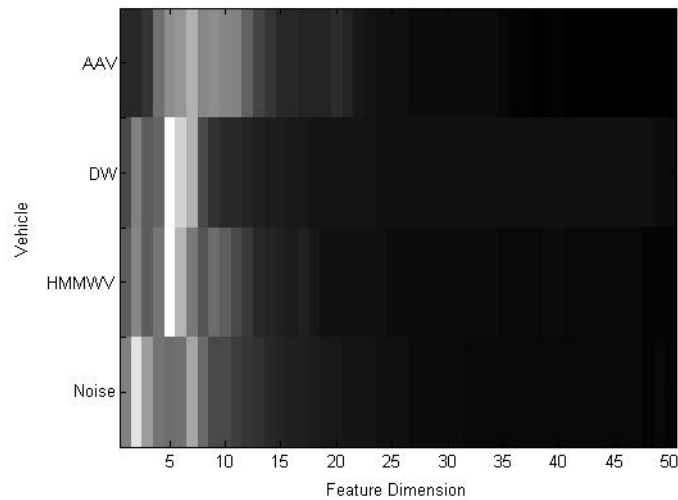


Fig. 3. Figure of typical normalized acoustic features for different vehicle classes.

Since the original acoustic time series contains both the acoustic signal sensed from the moving vehicle as well as background noise, the probability of correct classification may vary as the signal to noise ratio changes. It is intuitive to predict that if a sensor node is far away from the target vehicle, its SNR is lower, and hence the probability of correct classification will be lower. This is particularly easy to explain based on the maximum likelihood classifier architecture. In the ML classifier, we assume that the feature vector x is drawn from a conditional probability (*likelihood function*):

$$P(x|k) \sim \exp \left\{ \frac{-1}{2} (x - x_k)^T \Sigma_k^{-1} (x - x_k) \right\} . \quad (1)$$

where $x|k$ is the mean feature vector of k_{th} type of vehicle and Σ_k is the covariance matrix estimated from the training data samples. The ML classifier determines that x belongs to the k^* class of vehicle if $P(x|k^*) > P(x|k)$ for any $k \neq k^*$. As x is perturbed with higher background noise, it is more likely that the margin

$$P(x|k^*) - \max_{k \neq k^*} (P(x|k)) . \quad (2)$$

will shrink. As such, the probability of misclassification will increase. The level of noise can be determined calculating the signal to noise ratio SNR_{dB}, and should be inversely proportional to the distance between the node and the vehicle. To validate this conclusion, we conducted an experiment using a portion of the Sitex02 data set that was recorded when a vehicle is cruising across the east-west segment of the road in the sensor field. With the ground-truth data, we calculate the relative average distance between each sensor to the vehicle as well as the SNR_{dB} for each node during each 0.75-second interval. We also perform target classification using the FFT spectrum of the acoustic signal during that interval, and record the classification result based on Distance and SNR_{dB}.

Then, we collect such results for all the nodes in both regions that cover the road segment and compiled them into a histogram as shown in Figure 4. It is quite clear that as the target-sensor distance increases and the signal to noise ratio decreases, the probability of correct target classification decreases. In fact, this probability dropped below 0.5 when the target-sensor distance is greater than 100 meters. This empirically derived probability of correct classification will offer great information to facilitate the development of a distance-based, region-wide classification fusion method to be discussed in a moment.

Region-Based Information Fusion Within a short message submitted by individual sensor nodes to the manager node of the region, information is sent on the corresponding energy reading (a non-negative number), CFAR detection result (yes/no), classification result (one integer k), and detection results of PIR and seismic channels. Hence, its length is less than 30 bytes and would take little energy and bandwidth to transmit via the wireless channel.

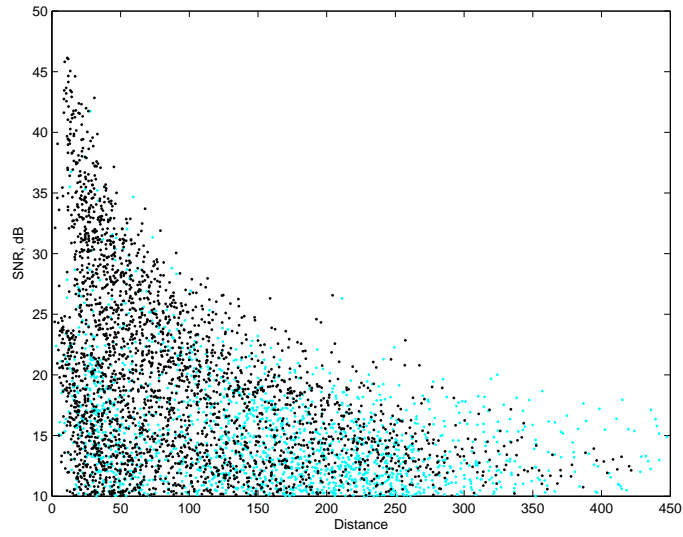


Fig. 4. Distribution of correct (*dark marks*) and incorrect (*light marks*) classifications based on distance and SNR_{dB}

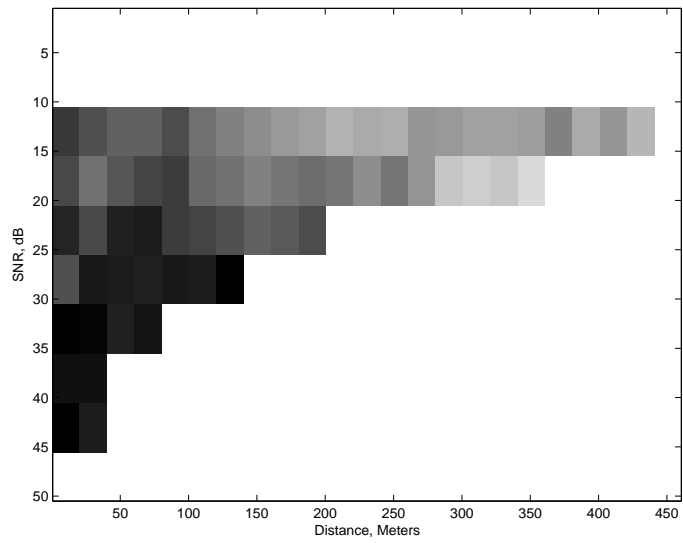


Fig. 5. Probability of correct target classification versus distance between sensor node and the target and the signal to noise ratio. Darker marks represent higher correct classification probability

At the region manager node, information fusion tasks will be performed. First, a region-wide detection decision will be made by majority votes from all sensor nodes that reported detection at any of the three sensing modality channels. If the sum of all these votes exceeds a preset threshold, it is deemed that there is indeed a vehicle present within the region. This will then trigger an energy-based target localization algorithm [5] to yield an estimate of the vehicle location. The location information then will be sent to a Kalman filter based tracking algorithm to facilitate data association, track filtering and track prediction. Details of these tasks will be reported in the near future.

3 Distance Based Classification Fusion

Apart from the localization and tracking of the target, it is also necessary to classify the type of vehicle within the region based on target classification results reported from member sensor nodes. Note that in our current system architecture, the target localization may be performed prior to region-wide target classification. Hence, if the target position is relatively accurate, it is possible to use the estimated target location and known sensor coordinates to calculate the target-sensor distance. Then, one may estimate the empirically derived probability of correct classification at a particular sensor node based on the distance information as described in section 3.

3.1 Data Fusion

Statistically speaking, data fusion [2] is the process of estimating the joint posterior probability (likelihood function in the uninformed prior case) based on estimates of the marginal posterior probability. Let $x(i)$ denote the feature vector observed at the i^{th} sensor node within the region, C_k denotes the k^{th} type of vehicle, the goal is to identify a function $f(\cdot)$ such that

$$P(x \in C_k | x(1), \dots, x(N)) \triangleq P(x \in C_k | \underline{x}) \approx f(g(P(x \in C_k | x(i))), 1 \leq i \leq N). \quad (3)$$

In our current work, we let the maximum function $g(z_k) = 1$ if $z_k > z_j$, $k \neq j$, and $g(z_k) = 0$ otherwise. Hence, our approach is known as *decision fusion*. Conventionally, there are two basic forms of the fusion function f .

Multiplicative Form If we assume that $x(i)$ and $x(j)$ are statistically independent feature vectors, then

$$P(x \in C_k | \underline{x}) = \prod_{i=1}^N P(x \in C_k | x(i)). \quad (4)$$

This approach is not realistic in the sensor network application and cannot be easily adapted to a decision fusion framework.

Additive Form The fusion function is represented as a weighted sum of the marginal posterior probability or local decisions:

$$\hat{P}(x \in C_k) = \sum_{i=1}^N w_i g_i(P(x \in C_k | x(i))) . \quad (5)$$

A baseline approach of region-based decision fusion would be simply choose $w_i = 1$ for $1 \leq i \leq N$. This would be called the *simple voting* fusion method.

3.2 Maximum A Posterior Decision Fusion

With distance-based decision fusion, we make each of the weighting factors w_i in equation 4 a function of distance and signal to noise ratio, that is $w_i = h(d_i, s_i)$ where d_i is the distance between the i^{th} sensor and the target and s_i is the signal to noise ratio defined as

$$\text{SNR}_{\text{dB}} = 10 \cdot \log_{10} \left(\frac{E_s - E_n}{E_n} \right) . \quad (6)$$

where E_s is the signal energy and E_n is the noise mean energy, both determined by the CFAR detection algorithm. We can use then the characterization gathered from the experiment referred in section 2 to formulate a Maximum A Posterior (MAP) Probability Gating network, using the Bayesian estimation

$$\hat{P}(x \in C_k) = P(x \in C_k | \underline{x}, d_i, s_i) \cdot P(\underline{x} | d_i, s_i) \cdot P(d_i, s_i) . \quad (7)$$

The prior probability $P(d_i, s_i)$ is the probability that the target is at the distance range d_i , and the acoustic signal SNR_{dB} is at the s_i range, and can be estimated empirically from the experiments. The conditional probability $P(\underline{x} | d_i, s_i)$ is also available from the empirically gathered data. With these, we may simply assign the following weights in eq. 5:

$$w_i = P(\underline{x} | d_i, s_i) \cdot P(d_i, s_i) . \quad (8)$$

In other words, if a particular sensor's classification result is deemed as less likely to be correct, it will be excluded from the classification fusion.

3.3 Nearest Neighbor Decision Fusion

It is desired to obtain fusion methods that will reduce the amount of information exchange required for decision making. Thus, it is logical to propose a method that will rely on as few node results as possible while maintaining acceptable results.

Let x, y be two **independent**, binary-valued random variables such that

$$P(x) = \begin{cases} a & \text{if } x = 1 \\ 1 - a & \text{if } x = 0 \end{cases} . \quad (9)$$

$$P(y) = \begin{cases} b & \text{if } y = 1 \\ 1 - b & \text{if } y = 0 \end{cases} . \quad (10)$$

where $0 \leq a, b \leq 1$, and $a > b$. Let

$$z = \text{sign}(cx + (1 - c)y - \theta) = \begin{cases} 1 & \text{if } cx - (1 - c)y > \theta \\ 0 & \text{otherwise} \end{cases} . \quad (11)$$

where $0 \leq \theta \leq 1$ is a threshold. Our goal is to find c , $0 \leq c \leq 1$, such that $P(z = 1)$ is maximized. Let us consider the four different combinations and the resulting values of $cx + (1 - c)y$:

$$cx + (1 - c)y = \begin{cases} 0 & \text{if } x = 0, y = 0 \\ 1 - c & \text{if } x = 0, y = 1 \\ c & \text{if } x = 1, y = 0 \\ 1 & \text{if } x = 1, y = 1 \end{cases} . \quad (12)$$

If $x = y = 1$ (with probability ab), $z = 1$. Also, if $x = 1, y = 0$ (with probability $a(1 - b)$), then $z = 1$ if $c \geq \theta$. Moreover, if $x = 0, y = 1$ (with probability $(1 - a)b$), then $z = 1$ if $c < \theta$. Since $a > b$, hence $a(1 - b) = a - ab > (1 - a)b = b - ab$. Therefore,

$$\begin{aligned} P(z = 1) &= P(x = 1, y = 1) + \begin{cases} P(x = 1, y = 0) & \text{if } c \geq \theta \\ P(x = 0, y = 1) & \text{if } c < \theta \end{cases} \\ &= \begin{cases} ab + a(1 - b) = a & \text{if } c \geq \theta \\ ab + (1 - a)b = b & \text{if } c < \theta \end{cases} . \end{aligned} \quad (13)$$

Since $a > b$, it is clear that the choice of c should be such that $c \geq \theta$. With θ varying between 0 and 1, the safest choice is $c = 1$, and it will yield the best performance.

To generalize the above result, denote $x_i : 1 \leq i \leq N$ to be N **independent**, binary-valued random variables with $P(x_i = 1) = a_i$. Suppose that $a_1 > a_i, i > 1$. Let

$$z = \text{sign} \left(\sum_{i=1}^N c_i x_i - \theta \right), \sum_{i=1}^N c_i = 1, 0 \leq c_i \leq 1 . \quad (14)$$

Then, the set of weights c_i that maximize the probability $z = 1$ will be

$$\underline{c} = [c_1 c_2 \dots c_N] = [1 \ 0 \dots 0] . \quad (15)$$

We have proved the case where $N = 2$. To prove using induction, suppose that the said vector will maximize the probability. For the $N + 1$ case, we want

to maximize $P(z = 1)$, and therefore, we want to maximize the sum of the $N + 1$ $c_i x_i$ terms.

As all c_i and x_i are positive, the sum will be maximum when its terms are maximum, which means that we can set $c_1 = 1$ and $c_i = 0$ for $2 \leq i \leq N$. However, we must note that $\sum_{i=1}^N c_i = 1$, and therefore, we can scale the N first coefficients to be

$$c'_i = \begin{cases} c_i(1 - c_{N+1}) & \text{for } 1 \leq i \leq N \\ c_{N+1} & \text{for } i = N + 1 \end{cases} . \quad (16)$$

This yields $c'_1 = 1 - c_{N+1}$, $c'_i = 0$ for $2 \leq i \leq N$, $c'_{N+1} = c_{N+1}$ and $\sum_{i=1}^N c_i = 1$. So we have two possibilities:

$$\sum_{i=1}^N c_i x_i = \begin{cases} 1 - c_{N+1} & x_i = 0 \\ 1 & x_i = 1 \end{cases} . \quad (17)$$

The expected value of this sum will be

$$\begin{aligned} E \left[\sum_{i=1}^N c_i x_i \right] &= a_i + (1 - c_{N+1})(1 - a_i) \\ &= 1 - c_{N+1} + c_{N+1} a_i \\ &= 1 - c_{N+1}(1 - a_i) . \end{aligned} \quad (18)$$

Since a_i is fixed, this value is maximum when c_{N+1} is minimum, which means $c_{N+1} = 0$ for an optimum case.

We now have another possible choice of w_i . That is,

$$w_i = \begin{cases} 1 & d_i < d_j, j \neq i \\ 0 & \text{otherwise} \end{cases} . \quad (19)$$

This choice of weights represents a nearest neighbor approach, where the result of the closest node to the target is assumed to be the region result.

We can use other choices that are functions only of distance. In this work, we use a simple threshold function:

$$w_i = \begin{cases} 1 & d_i \leq d_{max} \\ 0 & \text{otherwise} \end{cases} . \quad (20)$$

We compare these three different methods of choosing w_i to the baseline method of setting $w_i = 1$ for all i , and test them using seven different experiments in the Sitex02 data set, using one out of n training and testing. Our metrics are the classification rate and the rejection rate.

The classification rate is the ratio between the number of correctly classified samples and the total numbered of samples classified as vehicles. The rejection rate is the rate between the number of samples rejected by the classifier and the total number of samples ran through the classification algorithm. Consequently, the acceptance rate is the complement of the rejection rate.

There are two rejection scenarios with our current classifier scheme; one is at the node level, where one of the classes characterized during training collects typical samples of events with high energy that do not correspond to vehicles. These events are incorrectly detected and include such noises as wind, radio chatter and speech. The other is at the region level, where the region fusion algorithm does not specify satisfactorily a region classification result, i.e. no nodes were closer than d_{max} to the vehicle for the distance-based region fusion algorithm.

It is desired to obtain high classification rates while preserving low rejection rates. The results are listed in Tables 1 and 2. To analyze the impact of localization errors in the different methods, errors were injected to the ground truth coordinates following a zero-mean Gaussian distribution with several standard deviations. The results are shown in Tables 3 to 8.

Table 1. Classification rate fusion results using 4 methods

Fusion Method	MAP Bayesian	$d_{max} = 50$ m	Nearest Neighbor	Majority Voting
	77.19%	80.82%	83.55%	75.58%
AAV3	33.87%	50.79%	73.33%	27.12%
AAV6	100.00%	100.00%	100.00%	100.00%
AAV9	89.80%	90.63%	84.31%	91.84%
DW3	80.00%	83.78%	85.71%	82.50%
DW6	100.00%	100.00%	100.00%	100.00%
DW9	66.67%	75.00%	75.86%	63.33%
DW12	70.00%	65.52%	65.63%	64.29%

Table 2. Rejection rate fusion results using 4 methods

Fusion Method	MAP Bayesian	$d_{max} = 50$ m	Nearest Neighbor	Majority Voting
	9.53%	21.56%	7.40%	10.40%
AAV3	3.13%	1.56%	6.25%	7.81%
AAV6	4.29%	27.14%	2.86%	7.14%
AAV9	3.92%	37.25%	0.00%	3.92%
DW3	4.76%	11.90%	0.00%	4.76%
DW6	6.06%	9.09%	0.00%	0.00%
DW9	14.29%	31.43%	17.14%	14.29%
DW12	30.23%	32.56%	25.58%	34.86%

Table 3. Classification rate fusion results using 4 methods, and error injection with $\sigma = 12.5$ m

Fusion Method	MAP Bayesian	$d_{max} = 50$ m	Nearest Neighbor	Majority Voting
	77.14%	80.51%	81.89%	75.58%
AAV3	32.79%	56.45%	67.21%	27.12%
AAV6	100.00%	100.00%	100.00%	100.00%
AAV9	93.88%	90.63%	84.31%	91.84%
DW3	80.00%	81.08%	83.33%	82.50%
DW6	100.00%	100.00%	100.00%	100.00%
DW9	66.67%	78.26%	75.86%	63.33%
DW12	66.67%	57.14%	62.50%	64.29%

Table 4. Rejection rate fusion results using 4 methods, and error injection with $\sigma = 12.5$ m

Fusion Method	MAP Bayesian	$d_{max} = 50$ m	Nearest Neighbor	Majority Voting
	9.75%	22.32%	7.40%	10.40%
AAV3	4.69%	3.13%	6.25%	7.81%
AAV6	4.29%	25.71%	2.86%	7.14%
AAV9	3.92%	37.25%	0.00%	3.92%
DW3	4.76%	11.90%	0.00%	4.76%
DW6	6.06%	9.09%	0.00%	0.00%
DW9	14.29%	34.29%	17.14%	14.29%
DW12	30.23%	34.88%	25.58%	34.86%

Table 5. Classification rate fusion results using 4 methods, and error injection with $\sigma = 25$ m

Fusion Method	MAP Bayesian	$d_{max} = 50$ m	Nearest Neighbor	Majority Voting
	77.74%	79.42%	79.29%	75.56%
AAV3	37.70%	54.39%	55.36%	27.12%
AAV6	100.00%	100.00%	100.00%	100.00%
AAV9	89.80%	100.00%	88.24%	91.84%
DW3	80.00%	82.86%	80.95%	82.50%
DW6	100.00%	100.00%	100.00%	100.00%
DW9	66.67%	72.00%	72.41%	63.33%
DW12	70.00%	46.67%	58.06%	64.29%

Table 6. Rejection rate fusion results using 4 methods, and error injection with $\sigma = 25$ m

Fusion Method	MAP Bayesian	$d_{max} = 50$ m	Nearest Neighbor	Majority Voting
	9.75%	24.78%	8.63%	10.40%
AAV3	4.69%	10.94%	12.50%	7.81%
AAV6	4.29%	30.00%	2.86%	7.14%
AAV9	3.92%	50.98%	0.00%	3.92%
DW3	4.76%	16.67%	0.00%	4.76%
DW6	6.06%	6.06%	0.00%	0.00%
DW9	14.29%	28.57%	17.14%	14.29%
DW12	30.23%	30.23%	27.91%	34.88%

Table 7. Classification rate fusion results using 4 methods, and error injection with $\sigma = 50$ m

Fusion Method	MAP Bayesian	$d_{max} = 50$ m	Nearest Neighbor	Majority Voting
	77.74%	80.48%	76.72%	75.58%
AAV3	37.70%	51.28%	39.29%	27.12%
AAV6	100.00%	100.00%	100.00%	100.00%
AAV9	89.80%	95.00%	86.27%	91.84%
DW3	80.00%	84.62%	78.57%	82.50%
DW6	100.00%	95.24%	96.97%	100.00%
DW9	66.67%	72.22%	71.43%	63.33%
DW12	70.00%	65.00%	64.52%	64.29%

Table 8. Rejection rate fusion results using 4 methods, and error injection with $\sigma = 50$ m

Fusion Method	MAP Bayesian	$d_{max} = 50$ m	Nearest Neighbor	Majority Voting
	9.95%	46.01%	9.24%	10.40%
AAV3	4.69%	39.06%	12.50%	7.81%
AAV6	5.71%	45.71%	4.29%	7.14%
AAV9	3.92%	60.78%	0.00%	3.92%
DW3	4.76%	38.10%	0.00%	4.76%
DW6	6.06%	36.36%	0.00%	0.00%
DW9	14.29%	48.57%	20.00%	14.29%
DW12	30.23%	53.49%	27.91%	34.88%

3.4 Results and Analysis

For Tables 1 to 8, the cells that give the highest classification rate are highlighted, including tied cases. It is seen that Nearest Neighbor method yields out the best results consistently when the error is low or nonexistent - in 9 out of 14 cases. The distance-based and MAP-based methods give comparable results in cases where the error is larger (each method has the highest rate in 4 to 6 cases out of 14). However, the rejection rates are unacceptable for the distance-based method, even with nonexistent error, with an average of 35%.

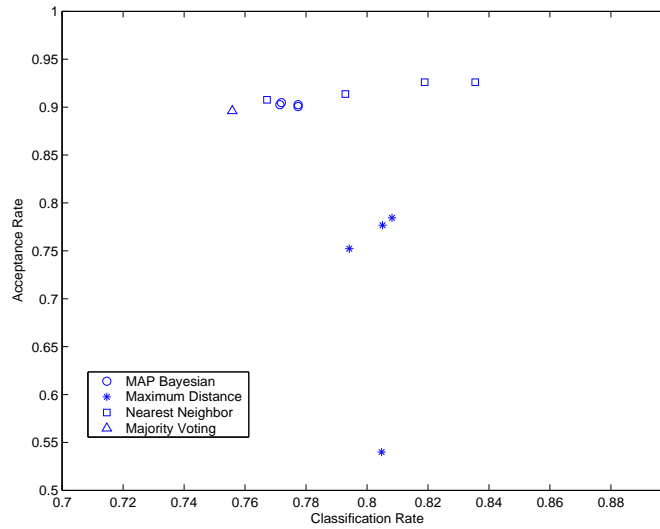


Fig. 6. Average classification and acceptance rate results for different classification region fusion methods

Figure 6 shows the average performance of the different methods for all the error injection scenarios. The results of the error impact experiments show that the MAP-based classification fusion is not heavily affected by the error injection; the change for the classification rate is less than 0.1% in average for an error injection up to $\sigma = 50$ m and the rejection rate increases 0.1% in average. The effects on the other methods are more pronounced, with a change of 3% in average in classification rate for the Nearest Neighbor method and an increase of 24% in the rejection rate of the distance-based method.

These experiments show higher classification rates for the MAP and Nearest Neighbor approaches while maintaining comparable acceptance rates. Further research is needed on additional considerations to avoid transmission of node classifications that have low probability of being correct; it is expected that the MAP-based method will easily allow for these additions.

4 Acknowledgment

This work was supported in part by DARPA under grant no. F 30602-00-2-0555.

References

1. Averbuch, A., Hulata, E., Zheludev, V., Kozlov, I.: A wavelet packet algorithm for classification and detection of moving vehicles. *Multidimensional Systems and Signal Processing* **12**, (2001) 9–31
2. Brooks, R. R., Iyengar, S. S.: *Multi-sensor fusion: fundamentals and applications with software*. Upper Saddle River, NJ: Prentice Hall PTR (1998)
3. Estrin, D., Girod, L. Pottie, G., Srivastava, M.: Instrumenting the world with wireless sensor network. *Proc. ICASSP'2001*. Salt Lake City, UT, (2001) 2675–2678.
4. Lennartsson, R. K., Pentek, A., Kadtke, J.B.: Classification of acoustic and seismic data using nonlinear dynamical signal models. *Proc. IEEE Workshop Statistical Signal and Array Processing* (2000) 722–726
5. Li, D., Hu, Y.H.: Energy Based Collaborative Source Localization Using Acoustic Micro-Sensor Array. *J. Applied Signal Processing*, pp. (to appear)
6. Li, D., Wong, K.D., Hu, Y. H., Sayeed, A. M.: Detection, classification and tracking of targets. *IEEE Signal Processing Magazine* **19** (2002) 17–29
7. Nooralahiyan, A. Y., Dougherty, M., McKeown, D., Kirkby, H.R.: A field trial of acoustic signature analysis for vehicle classification. *Transportation Research Part C* **5C** (1997) 165–177
8. Nooralahiyan, A.Y., Lopez, L., McKewon, D., Ahmadi, M.: Time-delay neural network for audio monitoring of road traffic and vehicle classification. *Proceedings of the SPIE*. (1997) 193–200
9. Nooralahiyan, A.Y., Kirby, H.R., McKeown, D.: Vehicle classification by acoustic signature. *Mathematical and Computer Modelling* **27** (1998) 205–214
10. Tung, T.L., Kung, Y.: Classification of vehicles using nonlinear dynamics and array processing. *Proceedings of the SPIE* (1999) 234–246